

Composite films prepared by immersion deposition of manganese oxide in carbon nanotubes grown on graphite for supercapacitors

Lingchuan Li · Khalid Lafdi

Received: 11 February 2011 / Accepted: 4 June 2011 / Published online: 16 June 2011
© Springer Science+Business Media, LLC 2011

Abstract Manganese oxide/carbon nanotube (CNT) composite films on graphite were prepared by growing CNTs on the substrate using chemical vapor deposition (CVD), followed by immersion in an aqueous solution of potassium permanganate. The CVD growth created favorable conditions for deposition of the oxide on the electrode, and an aligned porous structure of the composite films, which originated from the CNT growth, could be managed. Electrochemical behaviors of the CNT and the composite films for supercapacitors were studied in 1 M Na₂SO₄ solution. While the oxide deposition in the CNT films was identified as contributing to capacitance enhancement, it was also found that a mild heat treatment could improve performance of the composite films.

Introduction

Supercapacitors are energy storage and conversion devices that have a higher energy density than conventional capacitors, and a larger power density than batteries. There are two mechanisms to perform the energy storage and conversion: separation of electronic and ionic charge at the electrode/electrolyte interface and faradic redox reactions. The operation based on charge separation generally needs electrode materials of large surface area to provide the so called double-layer capacitance. Porous carbon materials, such as activated carbon, carbon aerogel, carbon nanotubes, etc., have been widely used and studied [1–3]. For electrochemical redox reaction operation, certain metal

oxides, and conducting polymers are usually utilized as the active materials because of their high pseudo-capacitance [4, 5].

Among various metal oxides, manganese oxide (MnO_x) is one of the most promising candidates for pseudo-capacitance, owing to its high-specific capacitance, abundance of manganese, low cost, and environmental friendliness. However, a major challenge from using the oxide in supercapacitors is its low electrical conductivity. To overcome this disadvantage, various approaches have been undertaken, such as engineering MnO_x with specific nanostructures [6, 7] or synthesizing MnO_x composites with conducting materials [8–11]. When utilized to form composites, carbon materials in their various forms, for example, mesoporous carbon, exfoliated graphite, and particularly carbon nanotubes (CNTs), can significantly increase electrochemical performance of MnO_x. It is the good electrical conductivity and porous structure of CNTs that contribute to the electrochemical improvement. The MnO_x/CNT composites are typically interesting for applications as positive electrode materials, coupled with activated carbon as a negative electrode material to form asymmetrical supercapacitors.

Chemical vapor deposition (CVD) is a known method of producing aligned CNT films that can reach millimeter scale thickness on certain substrates [12–15]. Using the in situ grown CNTs to make composite films, unique structures may be achieved. There have been only limited studies on using CNTs grown on electrically conducting substrates to form MnO_x/CNT composite films for supercapacitors [16–20]. Since electrochemical performance of MnO_x/CNT is not only determined by morphology and distribution of MnO_x in the composites but also the origin and texture of the carbon frame work, there is a need to investigate the composite films made using directly grown

L. Li (✉) · K. Lafdi
University of Dayton Research Institute, 300 College Park,
Dayton, OH 45469, USA
e-mail: lingchuan.li@notes.udayton.edu

CNTs. In addition, this approach may avoid employment of polymer binders that may introduce unnecessary charge transfer barriers at particle–particle and electrolyte–electrode interface to affect study.

The most studied way to prepare the composite films using the *in situ* grown CNTs is electrodeposition of MnO_x into the CNT films [17–20]. However, successful electrodeposition of the oxide deep into the CNT films requires that the CNT films are not dense and are very thin. For low packing density and vertically aligned CNT films, their diameter has to be sufficiently large to resist collapse from the aligned structure [20]. In addition, oxidative treatment may be required to improve wettability of the CNTs for better deposition [20]. In this study, dense CNTs were grown on a graphite substrate by CVD, and the composite films were prepared by simple immersion of the CNT films in a potassium permanganate solution.

Permanganate has a history of use as an oxidizer in the manufacture of organic chemicals. The primary redox reaction for permanganate is given as $\text{MnO}_4^- + 8\text{H}^+ + 5\text{e}^- \rightarrow \text{Mn}^{2+} + 4\text{H}_2\text{O}$. With excess permanganate, Mn^{2+} can be oxidized subsequently as $3\text{Mn}^{2+} + 2\text{MnO}_4^- + 2\text{H}_2\text{O} \rightarrow 5\text{MnO}_{2(s)} + 4\text{H}^+$, leading to formation of manganese oxide. More recently, permanganate solutions were used to purify CNTs, typically from amorphous carbon, with formation of manganese oxide that was usually removed by washing with the acids [21–23]. In this study, instead of removing the manganese oxide, its presence on CNTs was used to construct the aligned MnO_2/CNT composites. The electrochemical behavior of the composite films prepared was studied for supercapacitors, however, the composite films could also be interesting for other electrochemical devices.

Experimental

Graphite strips (K Technology, Langhome, PA) of size $30 \times 5 \times 1 \text{ mm}^3$ were cut for use. Prior to CNT growth, the graphite strips were electrodeposited with catalyst in an aqueous bath containing 10 mM iron and an additive. A tube furnace (Lindberg) that had a control over three heating zones was utilized to heat a quartz tube reactor of 22 mm diameter. During CVD process, the samples were kept at 800 °C in the reactor. A quartz boat carrying 0.05 g ferrocene powder was placed in front of the samples where temperature was about 150 °C. Acetylene (10 mL/min), hydrogen (30 mL/min), and argon (500 mL/min) were introduced into the quartz tube for the growth at atmospheric pressure. The thickness of the CNT films ranged from about 1–30 micrometers, dependent on the time of growth, which were between 1 and 10 min. The CNTs had

an average diameter about 25 nm as determined from images taken with a scanning electron microscope.

Before deposition of MnO_x , the CNT/graphite samples were immersed in 25% HNO_3 for 6 h to clean the catalyst impurity. Deposition of the oxide was implemented by immersing the CNT/graphite samples into 100 mL, 0.1 M, pH 8.3 aqueous solution of potassium permanganate (99%, Fisher Scientific) that was maintained at 70 °C by an isothermal water bath.

Morphology of the MnO_x/CNT was examined by Hitachi S-4800 high-resolution scanning electron microscope (HRSEM), operated at 15 kV. Elemental composition of the deposits was analyzed by an energy-dispersive X-ray spectrometer (EDS). The samples were characterized by X-ray diffraction (XRD) using a diffractometer (Rigaku Ultima III) with nickel-filtered $\text{Cu}-\text{K}\beta$ radiation ($\lambda = 1.5406 \text{ \AA}$). The diffraction patterns were taken at room temperature in the range of $10 < 2\theta < 80$ using step scans. Raman spectra were acquired using a Renishaw RA 100 Raman analyzer (1800 L/mm grating) in a backscattering geometry at room temperature in the range of 300–2000 cm^{-1} . The excitation source was a He–Ne laser at wavelength of 525 nm (1.96 eV). All spectra were collected with seven accumulations of 25 s each to gain a high signal/noise ratio. The measured spectra were analyzed using the Wire 2.0 software from Renishaw.

The electrochemical behaviors of the composite films were investigated by cyclic voltammetry (CV), and electrochemical impedance spectroscopy (EIS) techniques using a CHI 660C electrochemical working station (CH Instrument, Inc.) and a PARSTAT 2273 electrochemical system (Princeton Applied Science). All experiments were carried out in 1 M Na_2SO_4 aqueous solution at room temperature. A three-electrode system was employed, with a graphite strip as the counter electrode and Ag/AgCl (in 3 M KCl) as the reference electrode.

Results and discussion

Film characterization

SEM images for a CNT film about 25 μm thick are shown in Fig. 1a–d. The CNT film was immersed in the KMnO_4 solution for 60 min (Fig. 1b) and 720 min (Fig. 1c, d). As it can be seen, the CNTs were approximately aligned and perpendicular to the substrate, giving a porous structure that was favorable for access of the electrolyte. The immersion treatment did not cause collapse of the CNTs. The gaps between the CNTs were reduced at long immersion times due to deposition of the manganese oxide. After 720 min, the CNTs were solidly glued together and individual CNTs could only be seen at a torn part of the

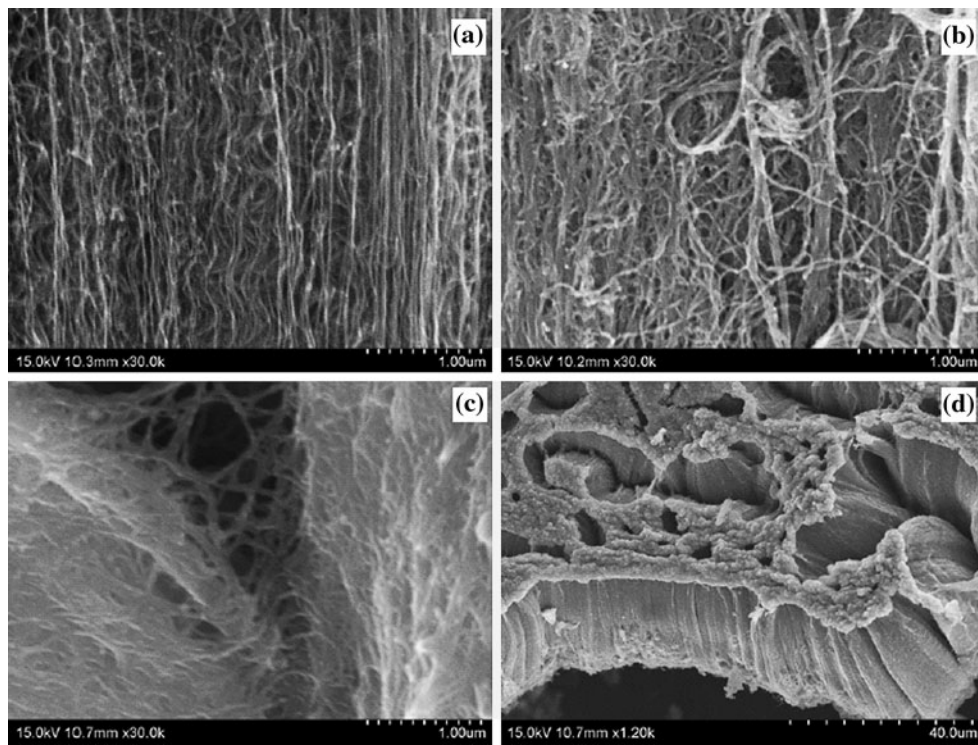


Fig. 1 Cross section images of a CNT film and its MnO_x/CNT composites: **a** prior to MnO_x deposition, **b** after MnO_x deposition for 60 min, **c** after MnO_x deposition for 720 min, **d** the low magnification image of (c)

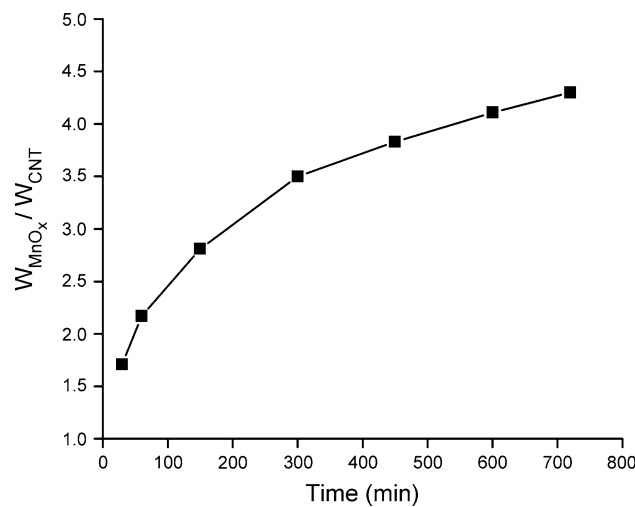


Fig. 2 Variation of MnO_x/CNT weight ratio as a function of immersion time

film (Fig. 1c). Examination at bottom, middle, and upper parts of the composite films proved that the deposition occurred uniformly. Figure 2 shows the variation of MnO_x/CNT mass ratio as a function of immersion time. A mass of MnO_x four times more than that of the original CNTs could be deposited in a 720 min immersion time.

Figure 3 shows the XRD patterns taken for a CNT film grown on the graphite substrate, and its composite film

prepared by immersion deposition. The sharp peaks at 26.6° , 54.8° , and 71.6° in the pattern of the CNT-grown graphite strip were identified to be from the substrate, with (002) plane of CNTs also contributing to the peak density at 26.6° . The broad diffuse peak around 45° was contributed by (100) and (101) of the CNTs. With an immersion in the potassium permanganate solution for 720 min, the peaks at 54.8° and 71.6° almost disappeared, while that at 26.6° was considerably weakened, indicating substantial deposition of the product. Owing to lack of clear new peaks, the product was likely amorphous in structure or poorly crystallized. EDS measurement revealed that Mn, O, and K were the major elements in the deposit, while C was detected for the CNTs (Fig. 4). The atomic ratio of O/Mn was in range of 1.8–2.5.

Figure 5 shows the Raman spectra of a CNT film at different stages of the MnO_x deposition. Prior to the immersion deposition, peaks from the CNTs were seen typically at 1350 (D-band) and 1593 cm^{-1} (G-band). Immersion for a time as short as 10 min gave a peak at $574\text{--}578 \text{ cm}^{-1}$, a shoulder at 640 cm^{-1} and two small peaks at $407\text{--}413 \text{ cm}^{-1}$ and $501\text{--}505 \text{ cm}^{-1}$. Increasing the immersion time to 60 min increased these peak and shoulder intensities. Further immersion in the solution up to 720 min resulted in not only substantial enhancement of peak density due to more deposition of the product, but also expansion in the band range and variation in shape. These spectra agree with

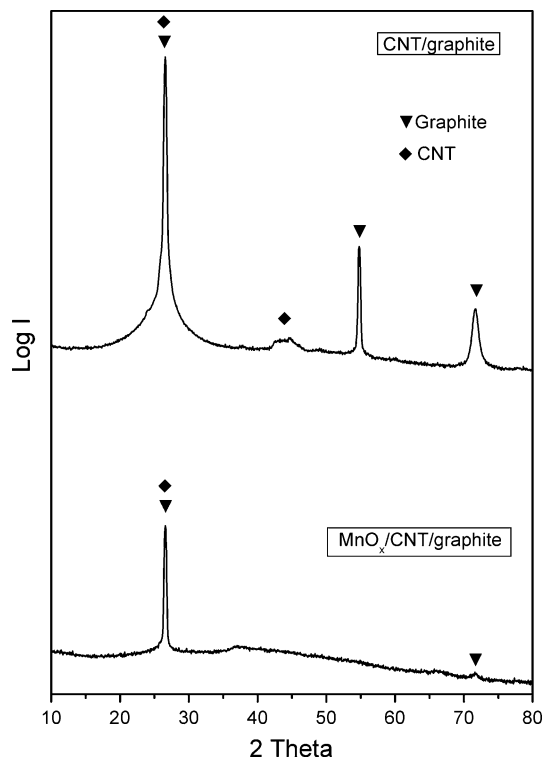


Fig. 3 XRD patterns of a CNT film on graphite and its composite counterpart

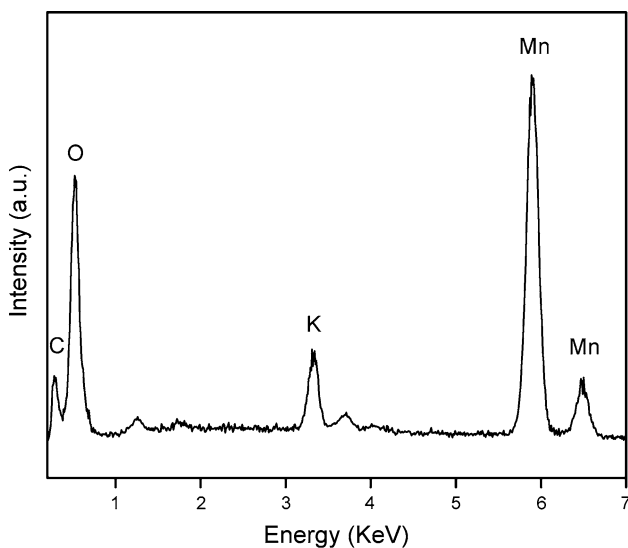


Fig. 4 EDS spectrum of a MnO_x/CNT film

general Raman scattering patterns of manganese oxide in that scattering at about 640 cm^{-1} could be related to symmetric stretching vibration (Mn–O) of MnO₆ groups, and the peaks around $574\text{--}578\text{ cm}^{-1}$ could be associated with Mn–O stretching vibration in the basal plane of MnO₆ sheet [24–27]. These peaks were different from those of potassium

permanganate, showing no the presence of the permanganate in the film except for its reduced product.

The peak density ratio of the D-band over the G-band of the CNTs, I_D/I_G , determined based on peak area, varied with the time of immersion deposition. Prior to the immersion treatment, I_D/I_G was 1.72. With 10 min immersion deposition, the ratio was significantly reduced to 1.20. This indicates that at the early stage of the immersion deposition, the oxide was formed primarily by oxidation of amorphous carbon in the CNT film. At immersion deposition time of 60 min, the profile of the two peaks was close to that of 10 min deposition, but the D-band peak started to rise again relative to the G-band peak ($I_D/I_G = 1.38$). This trend was more obviously shown for an extended immersion time of 720 min ($I_D/I_G = 1.79$). The relative rise of D-band peak starting from 60 min was considered to be correlated with defects in graphitic layers of the CNTs induced by the oxidant. This indicates that further deposition of the oxide would be from oxidation of the graphitic CNTs after consumption of amorphous carbon.

The presence of amorphous carbon might be beneficial for preparing the composites. First of all, significant presence of amorphous carbon on the walls of the CNTs should lead to considerable deposition of the manganese oxide before the CNTs were effectively attacked. Take the reaction of forming MnO₂ as an example, $4\text{MnO}_4^- + 3\text{C} + 2\text{H}_2\text{O} \rightarrow 4\text{MnO}_2 + 3\text{CO}_2 + 4\text{OH}^-$. Each gram of carbon would produce about ten grams of the oxide. Since physical properties, including electrical conductivity of CNTs, are inversely affected by their defects and damages, the proper presence of amorphous carbon would possibly lead to sufficient formation of the manganese oxide while protecting the CNTs from significant damage. Second, the presence of amorphous carbon in the depth of a CNT film might contribute to the uniform deposition of the oxide across the film thickness because of its lower oxidation resistance compared to the more graphitic carbon of CNTs.

Increasing immersion deposition time to 60 min increased peak and shoulder intensities of the manganese oxide (Fig. 5). Further immersion deposition up to 720 min resulted in not only substantial enhancement of peak density due to more deposition of the oxide, but also an expansion in the band range, indicating subtle change in the oxide, which could possibly result from a shift of the reductant from amorphous carbon to more graphitic CNTs that brought an alteration in valance ratio of manganese in the product.

Electrochemical behavior

The cyclic voltammograms (CV) recorded in 1 M Na₂SO₄ for a CNT film and its composite film prepared by

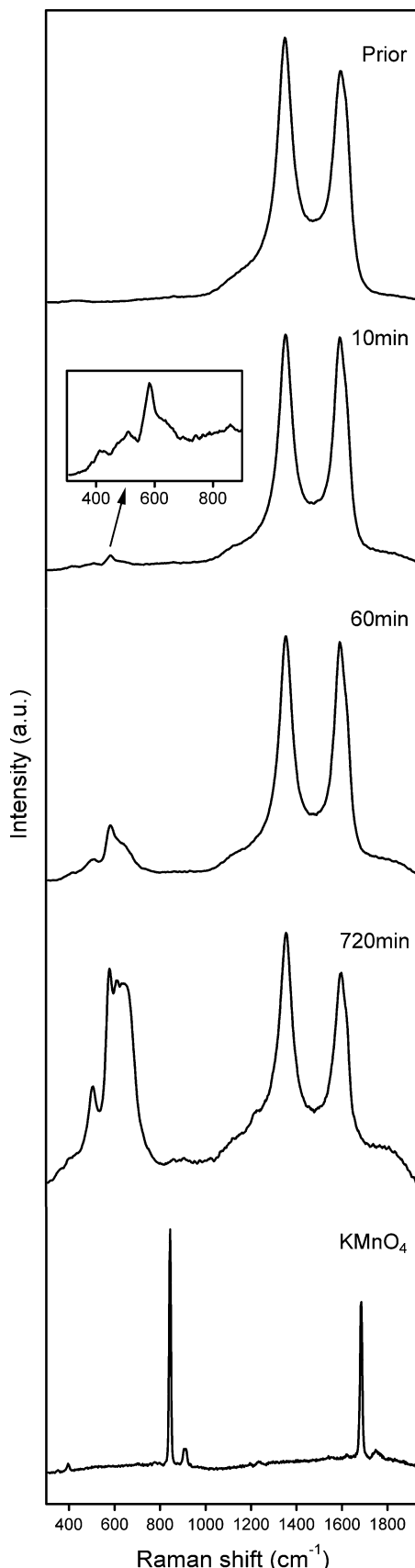
Fig. 5 Raman spectra of a CNT film and its composites made using ▶ the immersion deposition for 10, 60, and 720 min. That of KMnO_4 is given for comparison

deposition for 60 min in 1 M KMnO_4 are shown in Fig. 6. As it can be seen, the immersion deposition gave the CNT film a significant increase in current. The current of a graphite strip subjected to the same immersion treatment is also shown. The graphite strip had significantly lower current compared to the CNT and the composite films. It is concluded that the CNTs created more favorable conditions for deposition of the manganese oxide, i.e., availability of much larger surface area, existence of amorphous carbon, and possible lower oxidation resistance of the CNTs than the graphite strip.

For the as-prepared composite film, its current in the CV deviated from ideal rectangular shape. However, the heat treatment in air at 200 °C could significantly improve the electrochemical behavior, with its current shape being more rectangular and an increase in current value (Fig. 6). The result that current could be increased by the heat treatment is different from the case of a sole film of manganese oxide, where both decrease in the amount of hydrates and change in the valence states of manganese led to a reduction in current value [28]. For the composite films, effectiveness of the heat treatment was not only temperature related but also time dependent, with an optimized time about 60 min and a temperature at 200 °C.

Figure 7 shows Nyquist plots of EIS spectra recorded for a CNT film and its as-prepared and heat-treated composites. EIS measurements were carried out at open circle potential with a sinusoidal signal of 10 mV. At high frequency the impedance plots intersect with the real axis indicating R_s , which is a combination of ionic resistance, electronic resistance, contact resistance with the substrate, and connection resistance to the instrument. R_s of the CNT film was $4.58 \Omega \text{ cm}^2$, but it was increased to $6.58 \Omega \text{ cm}^2$ with deposition of the oxide. Apparently, the non-conducting nature of the manganese oxide and reduction of the pore volume in the film contributed to the increase of R_s . Heat treatment at 200 °C for a time as short as 10 min was effective to reduce the value of the composite film back to $6.24 \Omega \text{ cm}^2$, but the largest drop in R_s ($5.46 \Omega \text{ cm}^2$) was reached for a heating time of 60 min. Further extending the time raised R_s again, and for 120 min it was $7.02 \Omega \text{ cm}^2$. The improvement in CV of the composite film by the heat treatment was consequently associated with a possible change in contact status of MnO_x with the CNTs and the substrate that brought the above resistance difference.

At low frequencies, the Nyquist plot of an ideally polarizable capacitance should be a vertical line, while an inclined behavior can be related to electrode inhomogeneity



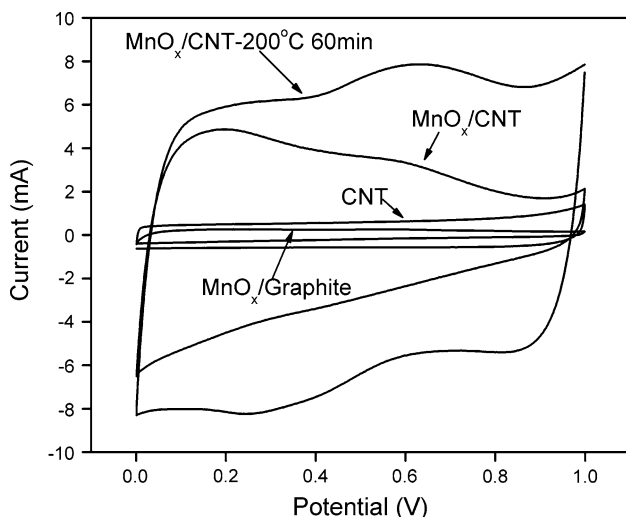


Fig. 6 Cyclic voltammograms of a CNT film, its as-prepared MnO_x /CNT composite, and the composite film heat treated at 200 °C for 60 min, in addition to that of a graphite strip that experienced the same immersion deposition in the KMnO_4 solution. *Electrolyte* 1 M Na_2SO_4 , scanning rate 5 mV/s

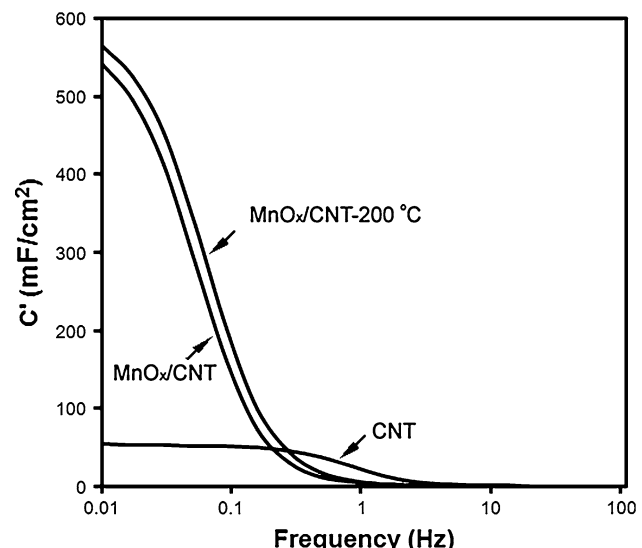


Fig. 8 Real capacitance versus frequency for a CNT film, its as-prepared composite, and the composite heated at 200 °C for 60 min. Deposition of MnO_x was performed in 1 M KMnO_4 for 60 min

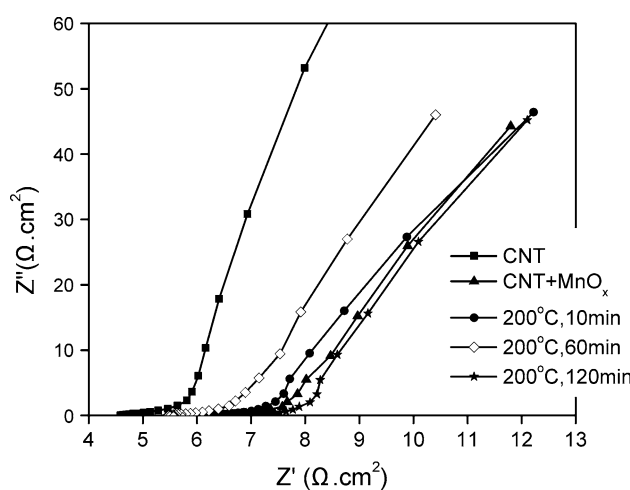


Fig. 7 Nyquist plots of a CNT film, its as-prepared composite, and the composite treated at 200 °C for 10, 60, and 120 min. Deposition of MnO_x was performed in 1 M KMnO_4 for 60 min

such as pore distribution. In Fig. 7, the CNT film had a slope closest to vertical in the low frequency region, where deposition of the manganese oxide caused more deviation in the slope. The heat treatment for 60 min significantly shifted the slope toward the vertical axis. This indicates that the heat treatment for the composite film affected its electrochemical properties by additionally changing pore distribution and size.

The impedance frequency behavior was studied using the complex model of the capacitance [29, 30]. The complex capacitance is expressed as follows:

$$C(\omega) = C'(\omega) - jC''(\omega) \quad (1)$$

where $C'(\omega)$ is the real part of the complex capacitance. The low frequency value of $C'(\omega)$ corresponds to the capacitance of the electrode at low scan or charge/discharge rate. $C''(\omega)$ is the imaginary part of the complex capacitance, and it stands for the energy dissipation by an irreversible process that leads to a hysteresis. $C'(\omega)$ and $C''(\omega)$ are given by,

$$C'(\omega) = -Z''(\omega)/(\omega|Z(\omega)|^2) \quad (2)$$

$$C''(\omega) = Z'(\omega)/(\omega|Z(\omega)|^2) \quad (3)$$

where $Z'(\omega)$ and $Z''(\omega)$ are the respective real and imaginary parts of the complex impedance $Z(\omega)$. ω is the angular frequency and it is given by $\omega = 2\pi f$.

Figures 8 and 9 show the variation of $C'(\omega)$ and $C''(\omega)$ with frequency. As it can be seen, deposition of the manganese oxide in the CNT film enhanced the real and imaginary parts of the complex capacitance. When the frequency was increased, $C'(\omega)$ decreased and at high frequency the supercapacitor behaved like a pure resistance. The change of $C'(\omega)$ with the frequency might depend on many parameters, such as the porous structure of the electrode, the electrode thickness, and the nature of the electrolyte. Corresponding to the energy dissipation, $C''(\omega)$ changed with the frequency but passed through a maximum. Compared to the as-prepared composite film, the heat treatment at 200 °C for 60 min, increased the value of $C'(\omega)$ at low frequency, and in the plot of $C''(\omega)$ versus frequency it shifted the peak to a higher frequency.

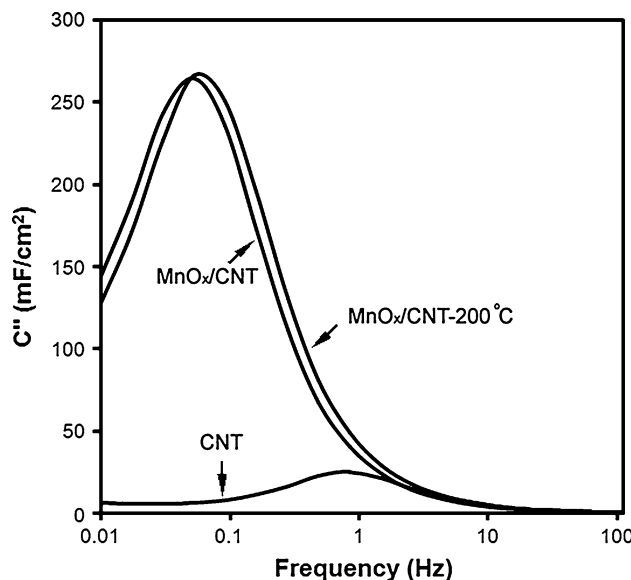


Fig. 9 Imaginary capacitance versus frequency for a CNT film, its as-prepared composite, and the composite heated at 200 °C for 60 min. Deposition of MnO_x was performed in 1 M KMnO_4 for 60 min

The relaxation time constant τ_0 , $\tau_0 = 1/f_0$, which is a figure of merit of a supercapacitor, can be determined from the plots of $C'(\omega)$ and $C''(\omega)$ versus frequency. For the real part of the complex capacitance, the relaxation time constant can be calculated from the frequency corresponding to the half of the maximum value of $C'(\omega)$. Moreover, the value of τ_0 can also be determined from the frequency where the imaginary part of the complex capacitance goes through a maximum. Deposition of the manganese oxide in the CNT film resulted in considerable increase of τ_0 from 1.2 s for the CNT film to 20.0 s for the as-prepared composite film. The heat treatment at 200 °C for 60 min, however, shifted τ_0 to a lower value of 17.7 s, giving some improvement.

Conclusions

The CNTs films directly grown on the conducting substrate by CVD created a possibility for preparing the MnO_x/CNT composite films simply by immersing the CNT films in the aqueous solution of KMnO_4 . By oxidizing the carbon impurities and the CNTs, MnO_x could be significantly and uniformly deposited in the CNT films. In addition to being a source of reductant, the CNTs provided surface area, mechanical support and pores for MnO_x deposition. The composite films so formed could preserve the aligned porous structure which originated from the CNT growth.

The aligned porous MnO_x/CNT composite films were amenable to heat treatment at a mild temperature. This led

to improvements in the electrochemical performance of the films for supercapacitors, including larger current value, more rectangular shape in CV, and reduction in the relaxation time constant. With such a porous and aligned structure, contact resistance of MnO_x with the CNTs and the substrate, as well as pore distribution and size, could be positively altered by the heat treatment, resulting in the improved electrochemical properties.

References

- Pandolfo AG, Hollenkamp AF (2006) J Power Sour 157:11
- Frackowiak E (2007) Phys Chem Chem Phys 9:1774
- Obreja VVN (2008) Physica E 40:2596
- Cottineau T, Toupin M, Delahaye T, Brousse T, Belanger D (2006) Appl Phys A 82:599
- Snook GA, Kao P, Best AS (2011) J Power Sour 196:1
- Zolfaghari A, Ataherian F, Ghaemi M, Gholami A (2007) Electrochim Acta 52(8):2806
- Xia H, Feng J, Wang H, Lai MO, Lu L (2010) J Power Sour 195:4410
- Reddy ALM, Shajumon MM, Gowda SR, Ajayan PM (2010) J Phys Chem C 114:658
- Wan C, Azumi K, Konno H (2007) Electrochim Acta 52:3061
- Malak-Polaczek A, Matei-Ghimbeu C, Vix-Guterl C, Frackowiak E (2010) J Solid State Chem 183:969
- Wang Y, Zhitomirsky I (2010) Colloids Surf A Physicochem Eng Aspects 369:211
- Eres G, Puretzky AA, Geohegan DB, Cui H (2004) Appl Phys Lett 84(10):1759
- Yun Y, Shanov V, Tu Y, Subramaniam S, Schulz MJ (2006) J Phys Chem B 110:23920
- Xiong GY, Wang DZ, Ren ZF (2006) Carbon 44:969
- Li Q, Zhang X, DePaula RF, Zheng L, Zhao Y, Stan L, Hollinger TG, Arendt PN, Peterson DE, Zhu YT (2006) Adv Mater 18:3160
- Fan Z, Chen J, Wang M, Cui K, Zhou H, Kuang Y (2006) Diam Relat Mater 15:1478
- Li L, Lafdi K (2009) In: Proceedings of SAMPE, Society for the advancement of material and process Engineering, Wichita
- Zhang H, Cao G, Wang Z, Yang Y, Shi Z, Gu Z (2008) Nano Lett 8(9):2664
- Wang Y, Liu H, Sun X, Zhitomirsky I (2009) Scripta Mater 61:1079
- Liu J, Essner J, Li J (2010) Chem Mater 22:5022
- Aitchison TJ, Ginic-Markovic M, Matisons JG, Simon GP, Fredericks PM (2007) J Phys Chem 111:2440
- Hernadi K, Siska A, Thien-Nga L, Forro L, Kiricsi I (2001) Solid State Ionics 141–142:203
- Hiura H, Ebbesen TW, Tanigaki K (1995) Adv Mater 7:275
- Ma SB, Ahn KY, Lee ES, Oh KH, Kim KB (2007) Carbon 45:375
- Feng Q, Kanoh H, Ooi K (1999) J Mater Chem 9:319
- Julien C, Massot M, Baddour-Hadjean R, Franger S, Bach S, Pereira-Ramos JP (2003) Solid State Ionics 159:345
- Julien CM, Massot M, Poinsignon C (2004) Spectrochim Acta Part A 60:689
- Chun SE, Pyun SI, Lee GJ (2006) Electrochim Acta 51:6479
- Ganesh V, Pitchumani S, Lakshminarayanan V (2006) J Power Sour 158:1523
- Portet C, Taberna PL, Simon P, Flahaut E (2005) J Power Sour 139:371